Photochemical & Photobiological Sciences

Accepted Manuscript

ROYAL SOCIETY OF CHEMISTRY

www.rsc.org/pps

Ultraviolet-activated persulfate oxidation of methyl orange: A comparison between artificial neural networks and factorial design for process modelling

Zacharias Frontistis[1,2*], Evroula Hapeshi[2], Despo Fatta-Kassinos[2], Dionissios Mantzavinos[1*]

[1]Department of Chemical Engineering, University of Patras, Caratheodory 1, University Campus, GR-26504 Patras, Greece

[2]Civil and Environmental Engineering Department and Nireas, International Water Research Center, University of Cyprus, P.O. Box 20537, 1678, Nicosia, Cyprus.

[*]Corresponding author. Tel.: +302610996136; fax: +30 2610969532
E-mail address: mantzavinos@chemeng.upatras.gr
[*]Corresponding author. Tel.: +302610996137; fax +30 2610969532
E-mail address: zfrontistis@chemeng.upatras.gr

Abstract

In this work, the degradation of azo dye methyl orange in model aqueous solutions byUVC light-inducedpersulfate oxidation was studied.Five operating parameters that mayinfluence decolorization kinetics were evaluated, namely, methyl orange (MO) (5-50 mg/L) and sodium persulfate (SPS) (50-150 mg/L) concentration, reaction time (up to 60 min), (un-buffered) solution pH (3-9) and the addition of NaCl (0-500 mg/L). The process was simulated applying and comparing two methodologies, namely a two-level factorial design and artificial neural networks (ANN).It was found thatMO concentration is the most influential parameter followed by the reaction time and SPS concentration, while solution pH and the addition of sodium chloride arestatisticallyless significant; this order of significance was predicted by both methodologies.ANNcan more accurately (i.e. in terms of R^2, MSE and residuals) simulate the process than factorial design, although they need significantly larger sets of data and computational time.

Keywords:process simulation;UVC/persulfate; azo dyes; decolorization; operating parameters

1. Introduction

Azo dyes and azo derivatives constitute about half of the global production of synthetic textile dyes because of their resistance to sunlight, water and other undesirable conditions. [1-3] Dye-containing effluents is an environmental concern since the color leads to visual pollution, while some dyes may have carcinogenic and/or teratogenic effects on public health. [1-4]Efficientdecolorization of wastewaters is one of the significant treatment problems as dyesare visible even at minute concentrations. Since most of the dyes are synthetic and designed to resist chemical and photochemical degradation, they are found to be resistant toconventional treatment processes.[1-6]

Methyl orange (MO) is a commonly used, water-soluble azo dye. In general, 15% of MO is released from dyeing operation processes and ultimately enters the waste stream.

In recent years, various efforts are being made to eliminate or effectively remove dyes; among them, advanced oxidation processes (AOPs) are a viable alternative option for the treatment of recalcitrant wastewaters.[7] The most common AOPs that have been applied for the decomposition of dyes include photocatalysis,[8-11] electrochemical oxidation,[12,13] ozone oxidation,[14-16]Fenton and photo-Fenton oxidation,[17,18] ultrasound[19,20]and the UV/H_2O_2 process.[21,22]

Just recently, sulfate radical-induced AOPs have gained increasing attention. The sulfate radical has a significantly high reduction potential of 2.6 V, slightly lower than that of hydroxyl radical (2.9 V).[23-26]Like the latter, it is non-selective and can quickly degrade most of the organic pollutants found in waters.[23,24]

One of the advantages of persulfate is that it can be activated in many ways including the presence of transition metals (usually iron), heat, microwaves, alkaline conditions or ultraviolet radiation.[23-26]

$$S_2O_8^{2-} \xrightarrow[\text{UV}]{\text{Heat}} 2SO_4^{\bullet-} \quad (1)$$

$$S_2O_8^{2-} + Fe^{2+} \longrightarrow SO_4^{\bullet-} + SO_4^{2-} + Fe^{3+} \quad (2)$$

$$S_2O_8^{2-} + 2H_2O \xrightarrow{OH^-} 3SO_4^{2-} + SO_4^{\bullet-} + O_2^{\bullet-} + 4H^+ \quad (3)$$

In recent years, there is a growing interest in the research community regarding theapplication of statistical methods for the simulation and optimization of AOPs.[27,28] Among them, the factorial design is often preferred due to a number of advantages such as simplicity, the relatively small number of experiments required and the possibility to interpret the physical meaning of the system.[27-30]On the other hand and as more and more computing power is becoming available, more complex, non-linear models,such as the artificial neural networks (ANN), are employedto simulate wastewater treatment.[31-33]

In this perspective, the objective of the present study was to investigate the degradation of MOin model aqueous solutions by UVC light-activated persulfate oxidationwith regard to identification of the key operating parameters that influence decolorization kinetics. This was done applyingand comparing two statistical approaches, namely factorial design and ANN.

2. Experimental and Analytical

2.1 Chemicals

Methyl Orange ($C_{14}H_{14}N_3NaO_3S$, CAS 547-58-0, Color Index Number: 13025)was purchased from Fluka and used as received. Sulfuric acid, sodium chloride and sodium hydroxide were purchased from Sigma-Aldrich, while sodium persulfate (SPS) was purchased from Riedel De Haen. Ultrapure water (Millipore) was used throughout the experimental procedure.

2.2 UVC photodegradation experiments

UVC irradiation was provided by a 9 W, low pressure mercury lamp (Radium, Puritec, UVC - LPC 9), which emits predominately at 254 nm.The photon flux of the lamp was determined actinometrically using 2-Nitrobenzaldehyde[34] and it was found equal to 4.57×10^{-6}einstein/s. The UVC lamp was placed inside a cylindrical quartz glass sleeve. UVC irradiation experiments were conducted in an immersion well, batch type, laboratory scale, cylindrical reaction vessel (length: 310 mm, internal diameter: 73 mm, volume capacity: 600 mL) purchased from Ace Glass (Vineland, NJ, USA). The reaction mixture was placed in the cylindrical reaction vessel and the UVC lamp, with its quartz glass sleeve, was immersed inside the reaction mixture. Temperature was left uncontrolled during the course of the reaction and it varied between 24ºC and 28ºC. The external reaction vessel was covered with aluminium foil to reflect radiation exerting the outer wall of the reaction vessel. In a typical run, 600 mL of the aqueous solution were introduced in the reaction vessel and the appropriate amount of sodium persulfate and/or sodium chloride when required, was added to achieve the desirable oxidant concentration in the range 50-150 mg/L.

The solution was magnetically stirred and subsequently the UVC lamp was turned on.

At specific time intervals about 2 mL of the reaction solution were withdrawn in vials which were immediately placed in an ice bath (4°C) to quench any further reactions.

2.1 Decolorization

MO concentration was followed on a JASCO V530 spectrophotometer. The extent of decolorization (Dec) that had occurred was computed as follows:

$$Dec = \frac{\int_{350}^{700} A_o - \int_{350}^{700} A_t}{\int_{350}^{700} A_o} \qquad (4)$$

whereA_o and A_t is the absorbance at t=0 and t=t, respectively averaged over the 350-700 nm range; this was done to minimize the effect of a possible spectrum shifting due to pH change during the reaction.

Total organic carbon (TOC) was measured by direct injection into an Aurora 1030 W TOC analyzer.

3. Results and discussion

3.1 Application of two-level factorial design

A statistical approach was chosen based on a factorial experimental design that would allow us to infer about the effect of the variables with a relatively small number of experiments.[27,28] The independent variables of the experimental design are presented in Table 1. Each one of the five variables received two values, a high value (indicated by the plus sign) and a low value (indicated by the minus sign).The substrate and oxidant concentration, reaction time and solution pH were chosen as independent variables since they typically affect the advanced oxidation of most organic contaminants, while NaCl was chosen since it constitutes a common chemical in dye-containing wastewaters. The range of these parameters was selected on the basis of preliminary experiments.

The experimental design followed in this work was a full 2^5 experimental set, which required 32 experiments. The order each experiment was performed was selected randomly and is shown in Table 2, along with values of each independent variable for each run. [27-29]

In this work, the Lenth's method was used for the assessment of the significance of the main and interaction effects in un-replicated factorial designs.[35]The method assumes that there are m independent effects, and that they all have the same variance. According to this method the pseudo-standard error (PSE) is estimated. First, the median of the absolute values of the effects is determined and then $s_0 = 1.5 \times$ median. Subsequently, any estimated effect

exceeding 2.5 × s_0 is excluded and the new median and PSE = 1.5 × median are calculated.[27,28]Once PSE has been obtained, it is multiplied by a factor $t_{0.95,d}$that is obtained from tables of quantiles of the t-distribution for common values of m and degrees of freedom, d = m/3, to estimate a margin of error (ME) for the effects.[27,28]

All estimated effects (given in Table 3) greater than the ME, in absolute values, are deemed significant. On the contrary, all other effects can be attributed to random statistical error.[27]

The Pareto chart is a useful presentation of the estimated effects and their statistical importance.[28,29] The Pareto chart displays the absolute values of the effects in a bar chart, as well as the decision line for the ME. The Pareto chart of the effects for the MO photodegradation is shown in Fig. 1. There are five effects that are greater than the ME decision threshold. Among them, the three most significant ones are the MO initial concentration, the treatment time and the concentration of sodium persulfate (SPS). Treatment time and sodium persulfate has a positive effect on decolorization. This means that an increase in their level brings about an increase in the MO degradation. However, MO initial concentration yields a negative effect regarding decolorization both as individual effect and through its interaction with time and sodium persulfate, indicating that an increase in its level brings about a decrease in the photodegradation of the dye. A decrease of conversion with increasing substrate concentration is common in most AOPs and denotes kinetics below first order (usually approaching zero order). In brief, this is due to the fact that the concentration of reactive radicals is finite for a fixed set of operating conditions and can be assumed constant during the early stages of the reaction.[36]At relatively high substrate-to-radicals concentration ratios, the latter are likely to become the limiting reactant, thus explaining the observed behaviour. As the reaction proceeds, this effect may become more pronounced due to the parallel, competitive reactions of transformation by-products with the non-selective radicals. Another consequence of the increased dye concentration has to do with the fact that the

solution becomes less permeable to UVC light and, consequently, less sodium persulfate reacts to generate sulphate radicals.[21] This is important since as can be seen in Fig. 1, an increase of sodium persulfate has a positive effect on decolorization.

According to the factorial design analysis both pH and sodium chloride appear to be statistically insignificant for process efficiency at least for the range of parameters studied. According to Bennedsenet al.[37] the presence of chloride can lead to different results since it can act either as radical scavenger or can participate in propagation reactions with oxidants and, thereby, not be entirely unproductive. The initial pH appears to have insignificant effect despite that fact that the production rate of sulphate radicals is pH-sensitive; however, as the solutions were not buffered to their initial pH values, pH either gradually dropped from basic to acidic or remained acidic during MO degradation, thus minimizing its effect.

Based on the variables and interactions, which are statistically significant, a model describing the experimental response of MO photodegradation was constructed(R^2=0.95) as follows:

$$\begin{aligned}\text{Dec (\%)} = &-0.2547\times X_1 + 0.0967\times X_2 + 0.1237\times X_5 \\ &-0.0882\times X_1\times X_5 - 0.0775\times X_1\times X_2 + 0.314\end{aligned} \quad (5)$$

where X_1, X_2 and X_3 are the transformed forms of the independent variables MO, SPS and time, respectively according to:

$$X_i = \frac{Z_i - \frac{Z_{high} + Z_{low}}{2}}{\frac{Z_{high} - Z_{low}}{2}} \quad (6)$$

andZ_i are the original, untransformed values.

Adequacy of the model was checked constructing the normal plot of residuals (Fig. 2).All points lie close to the straight line confirming that effects other that those considered in the model may be explained by random noise. [27-29]

It should be pointed out that the above linear model may be meaningful only for the range of conditions within which it has been developed. Since there are also other parameters that can influence the process (i.e. the water matrix including the presence of bicarbonates, residual

organic matter and other competitors for sulfate radicals), the above model should be used with particular caution.

Finally, the relative significance of the input variables was evaluated as follows and the results are summarized in Table 4:

$$\text{Relative significance} = \frac{|X_i|}{\sum |X_i|} \quad (7)$$

where X_i is the estimated effect for each significant variable according to the Pareto chart, while Σx_i is the sum of the effects of all significant variables (excluding the constant term).

3.2ANN modelling

A neural network consists of artificial neurons that are grouped into layers and interconnected in a variety of structures. The strength of these interconnections is determined by the weight associated with the neurons.[31-33] In this work, a three-layered back propagation ANN was chosen comprising an input layer (independent variables), an output layer (dependent variable) and a hidden layer. A tangent sigmoid (tansig) transfer function was employed to activate the hidden layer, while a linear (purelin) function for the input/output layers. The Levenberg-Marquardt back propagation algorithm was chosen for training purposes.[32,33]

The input layer includes five variables which are shown in Table 1 alongside the respective range of values, while MO decolorization is the dependent variable of the output layer. A set of 192 experimental data was divided into training (70%, 134 data), validation (15%, 29 data) and test (15%, 29 data) subsets in order to improve ANN generalization and to avoid a common problem related to ANN, i.e.overfitting. In this work the Neural Network Toolbox of Matlab R2011 mathematical software was employed for the prediction of MO degradation.

A crucial factor for the development of an ANN is the topology, i.e. the optimum number of neurons. This number can be derived minimizing the mean square error, MSE, which is defined as follows:

$$\mathrm{MSE} = \frac{\sum_{i=1}^{i=N} (y_{i,pred} - y_{i,exp})^2}{N} \qquad (8)$$

where$y_{i,pred}$ and $y_{i,exp}$ are the predicted and experimental values of the dependent variable, respectively and N is the number of data.

In this work, a trial and error approach was followed, i.e. a series of topologies were employed, in which the number of neurons was varied between 1 and 10. Each topology was repeated at least 10 times to avoid random correlation due to the random initialization of the weights. As seen in Fig.3, MSE is 0.0172for just one neuron and it is minimized to 0.00176 for five neurons; the resulting ANN is schematically illustrated in Fig. 4.

Fig. 5a shows a comparison between the measured MO decolorization and the predicted values to test the precision of the ANN model; there are two lines corresponding to (i) the perfect fit, y=x (i.e. experimental and predicted values would be identical), and (ii) the actual fit with a regression coefficient R^2=0.988, which implies a very good fit.

Finally, the relative significance of the input variables was evaluated using the neural weight matrix and the following equation proposed by Garson[38] and the results are summarized in Table 4.

$$Ij = \frac{\sum_{m=1}^{m=Nh} \left(\left(\left| w_{jm}^{ih} \right| / \sum_{k=1}^{Ni} \left| w_{km}^{ih} \right| \right) \times \left| w_{mn}^{ho} \right| \right)}{\sum_{k=1}^{k=Ni} \left\{ \sum_{m=1}^{m=Nh} \left(\left| w_{km}^{ih} \right| / \sum_{k=1}^{Ni} \left| w_{km}^{ih} \right| \right) \times \left| w_{mn}^{ho} \right| \right\}} \qquad (9)$$

Where I_j is the relative significance of the jth input variable on the output variable, N_i and N_h

are the numbers of input and hidden neurons, respectively and w is the connection weight. The subscripts k, m and n refer to input, hidden and output neurons, respectively, while the superscripts i, h and o refer to input, hidden and output layers, respectively. For the range of parameters studied, [MO] is the most influential variable (33.5%) followed by reactiontime (27.3%) and [SPS] (23.2%), while pH and sodium chloride concentration are far less significant for the process.

3.3Comparison between artificial neural networks and factorial design

Fig. 5b shows a comparison between the measured MO decolorization values and those predicted by the ANN and factorial design approaches for representative runs.From a strictly "mathematical" point of view (i.e. in terms of R^2, MSE and residuals),ANN simulate better the process, which is due to its non-linear behaviour, at least within the range of the operating parameters studied. In the case of the factorial design though, one should not ignore (i) the ease of interpretation of the results and the likely correlation with the physical meaning of the system under consideration, and (ii)the fact that reliable results can be produced using a very small number of experiments and measurements, thus saving time and reducing costs.

Although ANN are generally considered as black box in the literature, it is interesting to notice that the sensitivity analysis shown in Table 4gives exactly the same order of the significant factors for both ANN and factorial design. This is also true when the factorial design results are re-analyzed ignoring all interactions (i.e. simple first order analysis). This is an indication that ANN can also be used to provide some valuable information about the nature of the system and not only as a tool to simulate and predict data series.

4. Conclusions

The major conclusions drawn from this study are summarized as follows:

- Process simulation was performed by means of factorial design and artificial neural networks. Methyl orange concentration is the most important parameter followed by the reaction time and sodium persulfate concentration, while the pH and the addition of sodium chloride appear to be statistically less significant

- UVC/SPS is an effective process for the degradation of methyl orange.The optimal values of the operating parameters at the experimental conditions in question were found to be: [MO]=5 mg/L, [SPS]=150 mg/L, pH=3, without addition of sodium chloride and 10 min of treatment time. The decolorization of MO approached 100% under optimal conditions, while the TOC removal was 60%.The UV/SPS process seems to be competitive to otherphoto-assisted AOPs like the photo-Fenton process [17], where the time needed to achieve the degradation of 10 mg/L MO was 15 minand the UV/H_2O_2process [22] where the time needed to degrade 20 mg/L of the azo dye reactive orange 16 in the presence of 25 mmol/L $H_2O_2$was 20 min.

- Artificial neural networks have better performance than factorial design for the simulation of the process (R^2=0.988 and 0.95for ANN and two-level factorial design, respectively), although they need significantly larger sets of data (i.e. 192 data points versus 32 for factorial design) and computational time.

- Interestingly, the sensitivity analysis concerning the significance of the studied variables gives comparable results for both methodologies.

Acknowledgements

Nireas-International Water Research Center (NEA UPODOMH/STPATH/0308/09) is co-financed by the Republic of Cyprus and the European Regional Development Fund through the Research Promotion Foundation of Cyprus.

References

1. E. Forgacs, T. Cserhati, and G. Oros, Removal of synthetic dyes from wastewaters: A review,*Environ. Int.*, 2004, **30**, 953–971.

2. K. Singh and S. Arora, Removal of Synthetic Textile Dyes From Wastewaters: A Critical Review on Present Treatment Technologies,*Crit. Rev. Environ. Sci. Technol.*, 2011, **41**, 807–878.

3. A. B. dos Santos, F. J. Cervantes, and J. B. van Lier, Review paper on current technologies for decolourisation of textile wastewaters: Perspectives for anaerobic biotechnology,*Bioresour. Technol.*, 2007, **98**, 2369–2385.

4. C. Allegre, P. Moulin, M. Maisseu, and F. Charbit, Treatment and reuse of reactive dyeing effluents, *J. Memb. Sci.*, 2006, **269**, 15–34.

5. T. A. Nguyen and R. S. Juang, Treatment of waters and wastewaters containing sulfur dyes: A review*Chem. Eng. J.*, 2013, **219**, 109–117.

6. T. Robinson, G. McMullan, R. Marchant, and P. Nigam, Remediation of dyes in textile effluent: a critical review on current treatment technologies with a proposed alternative, *Bioresour. Technol.*, 2001, **77**, 247–255.

7. C. Comninellis, A. Kapalka, S. Malato, S. A. Parsons, I. Poulios, and D. Mantzavinos, Advanced oxidation processes for water treatment: advances and trends for R&D,*J. Chem. Technol. Biotechnol.*, 2008, **83**, 769–776.

8. P. A. Pekakis, N. P. Xekoukoulotakis, and D. Mantzavinos, Treatment of textile dyehouse wastewater by TiO_2 photocatalysis,*Water Res.*, 2006, **40**, 1276–1286.

9. I. Arslan, I. A. Balcioglu, and D. W. Bahnemann, Heterogeneous photocatalytic treatment of simulated dyehouse effluents using novel TiO_2-photocatalysts, *Appl. Catal. B Environ.*, 2000, **26**, 193–206.

10. E. Chatzisymeon, C. Petrou and D. Mantzavinos, Photocatalytic treatment of textile dyehouse effluents with simulated and natural solar light,*Global Nest J.*, 2013, **15**, 21-28.

11. D. E. Kritikos, N. P. Xekoukoulotakis, E. Psillakis, and D. Mantzavinos, Photocatalytic degradation of reactive black 5 in aqueous solutions: Effect of operating conditions and coupling with ultrasound irradiation,*Water Res.*, 2007, **41**, 2236–2246.

12. E. Chatzisymeon, N. P. Xekoukoulotakis, A. Coz, N. Kalogerakis, and D. Mantzavinos, Electrochemical treatment of textile dyes and dyehouse effluents,*J. Hazard. Mater.*, 2006, **137**, 998–1007.

13. E. Tsantaki, T. Velegraki, A. Katsaounis, and D. Mantzavinos, Anodic oxidation of textile dyehouse effluents on boron-doped diamond electrode,*J. Hazard. Mater.*, 2012,**207-208**, 91–96.

14. J. Wu and T. Wang, Ozonation of aqueous azo dye in a semi-batch reactor,*Water Res.*, 2001, **35**, 1093–1099.

15. L. W. Lackey, R. O. Mines, and P. T. McCreanor, Ozonation of acid yellow 17 dye in a semi-batch bubble column,*J. Hazard. Mater.*, 2006, **138**, 357–362.

16. K. Turhan and Z. Turgut, Decolorization of direct dye in textile wastewater by ozonization in a semi-batch bubble column reactor,*Desalination*, 2009, **242**, 256–263.

17. L. Gomathi Devi, S. Girish Kumar, K. Mohan Reddy, and C. Munikrishnappa, Photo degradation of Methyl Orange an azo dye by Advanced Fenton Process using zero valent

metallic iron: Influence of various reaction parameters and its degradation mechanism,*J. Hazard. Mater.*, 2009, **164**, 459–467.

18. S. P. Sun, C. J. Li, J. H. Sun, S. H. Shi, M. H. Fan, and Q. Zhou, Decolorization of an azo dye Orange G in aqueous solution by Fenton oxidation process: Effect of system parameters and kinetic study, *J. Hazard. Mater.*, 2009, **161**, 1052–1057.

19. H. Zhao, G. Zhang, and Q. Zhang, MnO_2/CeO_2 for catalytic ultrasonic degradation of methyl orange,*Ultrason. Sonochem.*, 2014, **21**, 991–996.

20. L. Wang, L. Zhu, W. Luo, Y. Wu, and H. Tang, Drastically enhanced ultrasonic decolorization of methyl orange by adding CCl_4,*Ultrason. Sonochem.*, 2007, **14**, 253–258.

21. S. Haji, B. Benstaali, and N. Al-Bastaki, Degradation of methyl orange by UV/H_2O_2 advanced oxidation process,*Chem. Eng. J.*, 2011, **168**, 134–139.

22. J. Mitrovic, M. Radovic, D. Bojic, T. Andjelkovic, M. Purenovic, and A. Bojic, Decolorization of textile azo dye reactive orange 16 with UV/H_2O_2 process,*J. Serbian Chem. Soc.*, 2012, **77**, 465–481.

23. G. Subramanian, P. Parakh, and H. Prakash, PDT photoinactivation of bacteria by visible light activation of persulphate using a tris(2,2'-bipyridyl)ruthenium(II) complex,*Photochem. Photobiol. Sci.*, 2013, **12**, 456–66.

24. S. Yang, P. Wang, X. Yang, L. Shan, W. Zhang, X. Shao, and R. Niu, Degradation efficiencies of azo dye Acid Orange 7 by the interaction of heat, UV and anions with common oxidants: Persulfate, peroxymonosulfate and hydrogen peroxide,*J. Hazard. Mater.*, 2010, **179**, 552–558.

25. Y. T. Lin, C. Liang, and J. H. Chen, Feasibility study of ultraviolet activated persulfate oxidation of phenol,*Chemosphere*, 2011, **82**, 1168–1172.

26. Y. Gao, N. Gao, Y. Deng, Y. Yang, and Y. Ma, Ultraviolet (UV) light-activated persulfate oxidation of sulfamethazine in water,*Chem. Eng. J.*, 2012, **195-196**, 248–253.

27. E. Chatzisymeon, N. P. Xekoukoulotakis, and D. Mantzavinos, Determination of key operating conditions for the photocatalytic treatment of olive mill wastewaters,*Catal. Today*, 2009, **144**, 143–148.

28. E. Chatzisymeon, N. P. Xekoukoulotakis, E. Diamadopoulos, A. Katsaounis, and D. Mantzavinos, Boron-doped diamond anodic treatment of olive mill wastewaters: Statistical analysis, kinetic modeling and biodegradability,*Water Res.*, 2009, **43**, 3999–4009.

29. A. Katsoni, Z. Frontistis, N. P. Xekoukoulotakis, E. Diamadopoulos, and D. Mantzavinos, Wet air oxidation of table olive processing wastewater: Determination of key operating parameters by factorial design,*Water Res.*, 2008, **42**, 3591–3600.

30. Z. Frontistis, D. Fatta-Kassinos, D. Mantzavinos, and N. P. Xekoukoulotakis, Photocatalytic degradation of 17α-ethynylestradiol in environmental samples by ZnO under simulated solar radiation,*J. Chem. Technol. Biotechnol.*, 2012, **87**, 1051–1058.

31. Z. Frontistis, V. M. Daskalaki, E. Hapeshi, C. Drosou, D. Fatta-Kassinos, N. P. Xekoukoulotakis, and D. Mantzavinos,Photocatalytic (UV-A/TiO2) degradation of 17α-ethynylestradiol in environmental matrices: Experimental studies and artificial neural network modeling,*J. Photochem. Photobiol. A Chem.*, 2012, **240**, 33–41.

32. Z. Frontistis, C. Drosou, K. Tyrovola, D. Mantzavinos, D. Fatta-Kassinos, D. Venieri, and N. P. Xekoukoulotakis,Experimental and modeling studies of the degradation of

estrogen hormones in aqueous TiO_2 suspensions under simulated solar radiation,*Ind. Eng. Chem. Res.*, 2012, **51**, 16552–16563.

33. A. R. Khataee and M. B. Kasiri,Artificial neural networks modeling of contaminated water treatment processes by homogeneous and heterogeneous nanocatalysis,*J. Mol. Catal. A Chem.*, 2010, **331**, 86–100.

34. E. S. Galbavy, K. Ram, and C. Anastasio, 2-Nitrobenzaldehyde as a chemical actinometer for solution and ice photochemistry, *J. Photochem. Photobiol. A Chem*., 2010, **209**, 186–192.

35. R. Lenth, Quick and easy analysis of unreplicated factorials,*Technometrics*, 1989, **31**, 469–473.

36. D. Dimitrakopoulou, I. Rethemiotaki, Z. Frontistis, N. P. Xekoukoulotakis, D. Venieri, and D. Mantzavinos,Degradation, mineralization and antibiotic inactivation of amoxicillin by UV-A/TiO_2 photocatalysis,*J. Environ. Manage*., 2012, **98**, 168–174.

37. L. R. Bennedsen, J. Muff, and E. G. Soogaard, Influence of chloride and carbonates on the reactivity of activated persulfate,*Chemosphere*, 2012, **86**, 1092–1097.

38. G.D. Garson, Interpreting neural-network connection weights,*AI Expert*, 1991, **6**, 46–51.

Table 1. Range of the factorial design and ANN input variables used in this work.

Input variable	Factorial design	ANN
[Methyl orange]	5 – 50 mg/L	5 – 50 mg/L
[Sodium persulfate]	50 – 150 mg/L	50 – 150 mg/L
Reaction time	3 – 10 min	0 – 60 min
pH	3 – 9	3 – 9
[Sodium Chloride]	0 – 500 mg/L	0 – 500 mg/L

Table 2. Design matrix of the 2^5 factorial design and observed response.

Order of running experiments	Level value of each variable in the experimental run					Decolorization (%)	
	MO_0	SPS_0	pH_0	NaCl	Time	Measured (experimental) value	Factorial Model
22	-	-	-	-	-	0.149	0.246
11	+	-	-	-	-	0.020	0.023
3	-	+	-	-	-	0.666	0.541
27	+	+	-	-	-	0.034	0.008
12	-	-	+	-	-	0.148	0.111
10	+	-	+	-	-	0.026	-0.012
21	-	+	+	-	-	0.485	0.534
20	+	+	+	-	-	0.021	0.102
19	-	-	-	+	-	0.331	0.272
5	+	-	-	+	-	0.019	0.039
32	-	+	-	+	-	0.345	0.503
13	+	+	-	+	-	0.025	-0.040
23	-	-	+	+	-	0.138	0.144
31	+	-	+	+	-	0	0.011
2	-	+	+	+	-	0.589	0.503
25	+	+	+	+	-	0.042	0.060
7	-	-	-	-	+	0.673	0.669
18	+	-	-	-	+	0.056	0.093
8	-	+	-	-	+	1	1.007
30	+	+	-	-	+	0.108	0.121
14	-	-	+	-	+	0.420	0.477
4	+	-	+	-	+	0.113	0.001
17	-	+	+	-	+	0.983	0.942
9	+	+	+	-	+	0.112	0.157
29	-	-	-	+	+	0.859	0.712
24	+	-	-	+	+	0.069	0.126
28	-	+	-	+	+	0.910	0.986
1	+	+	-	+	+	0.125	0.089
26	-	-	+	+	+	0.435	0.526
6	+	-	+	+	+	0.014	0.040
15	-	+	+	+	+	0.963	0.927
16	+	+	+	+	+	0.159	0.132

Table 3. Estimated effects of the 2^5 factorial design for MO photodegradation.

Effect	MO photodegradation
Average effect	0.3140
Main effects	
MO	-0.5093
SPS	0.1935
pH	-0.0463
NaCl	0.0006
Reaction time	0.2475
Two-factor interactions	
MO X SPS	-0.1549
MO X pH	0.0503
MO X NaCl	-0.0052
MO X Reaction Time	-0.1765
SPS X pH	0.0641
SPS X NaCl	-0.032
SPS X Reaction time	0.0212
pH X NaCl	0.0033
pH X Reaction time	-0.0289
NaCl X Reaction time	0.0081
Three-factor interactions	
MO X SPS X pH	-0.0574
MO X SPS X NaCl	0.0555
MO X SPS X Reaction time	0.0029
MO X pH X NaCl	-0.0132
MO X pH X Reaction Time	0.0349
MO X NaCl X Reaction Time	-0.0088
SPS X pH X NaCl	0.0661
SPS X pH X Reaction Time	0.0297
SPS X NaCl X Reaction Time	0.0117
pH X NaCl X Reaction Time	-0.0263
Four-factor interactions	
MO X SPS X pH X NaCl	-0.0412
MO X SPS X pH X Reaction Time	-0.0273
MO X SPS X NaCl X Reaction Time	0.0021
MO X pH X NaCl X Reaction Time	0.0156
SPS X pH X NaCl X Reaction Time	-0.0182
Five-factor interactions	
MO X SPS X pH X NaCl X Time	0.0290
Lenth's PSE	0.0401788

Table 4. Relative significance of the input variables.

Input variable	Factorial design	Factorial design (no interactions)	ANN
[MO]	38%	50.1%	33.5%
[Sodium persulfate]	15%	19.2%	23.2%
Reaction time	18%	24.7%	27.3%
pH	3%	4.7%	8%
[NaCl]	0.3%	0.3%	8%
[MO] x Time	14%	-	-
[MO] x [Sodium persulfate]	12%	-	-

List of figures

Figure 1. Pareto chart of the effects for MO photodegradation. White bars: positive effects; hatched bars: negative effects. The line is drawn at the margin of error (ME).

Figure 2. Normal probability plot of the residuals at 95% confidence interval for MO photodegradation.

Figure 3. Optimization of number of neurons in relation to MSE.

Figure 4. Structure of the optimized ANN used in this work.

Figure 5. Comparison between measured and predicted values of the dependent variable. (a) ANN; (b) ANN versus factorial design.

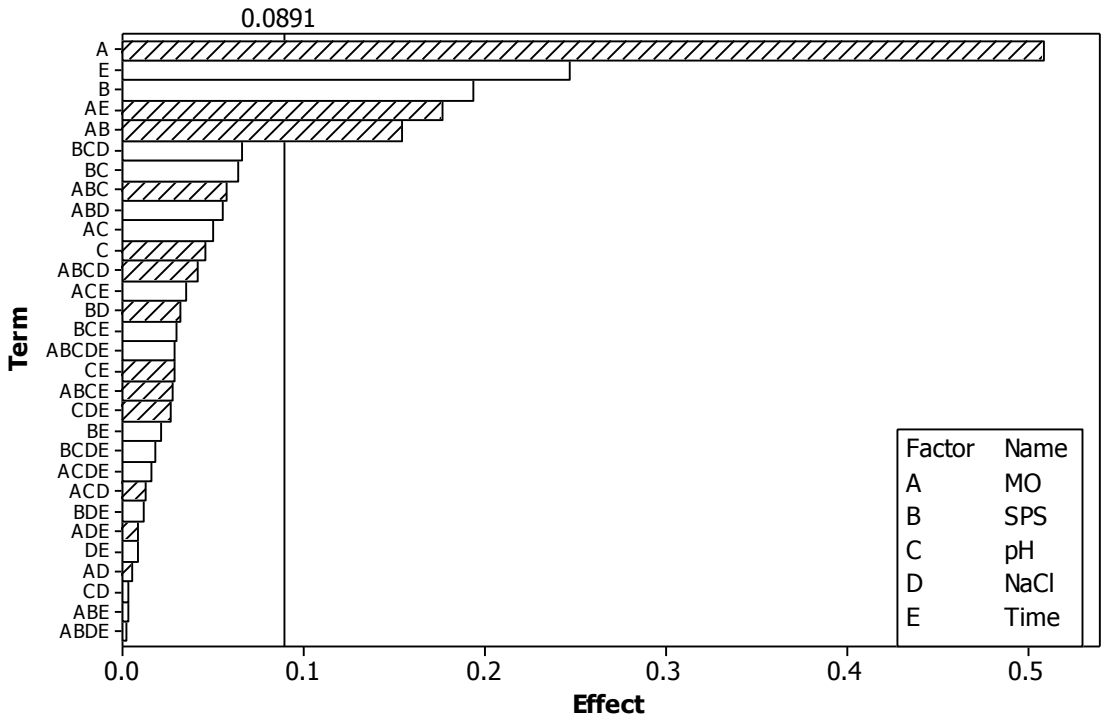

Figure 1. Pareto chart of the effects for MO photodegradation. White bars: positive effects; hatched bars: negative effects. The line is drawn at the margin of error (ME).

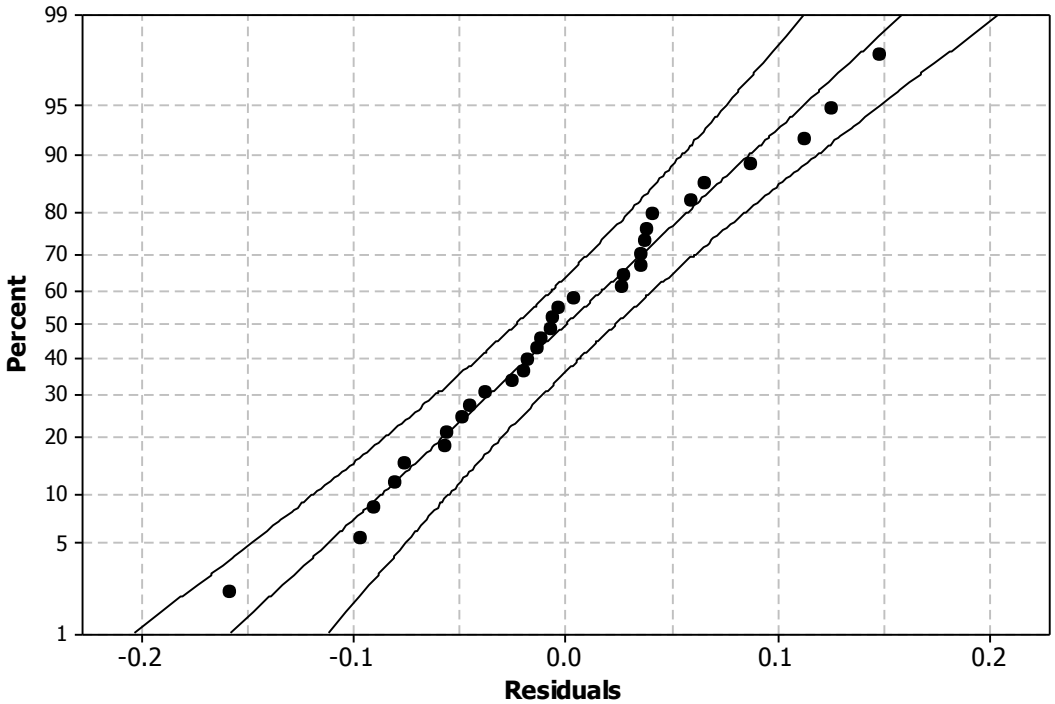

Figure 2. Normal probability plot of the residuals at 95% confidence interval for MOphotodegradation.

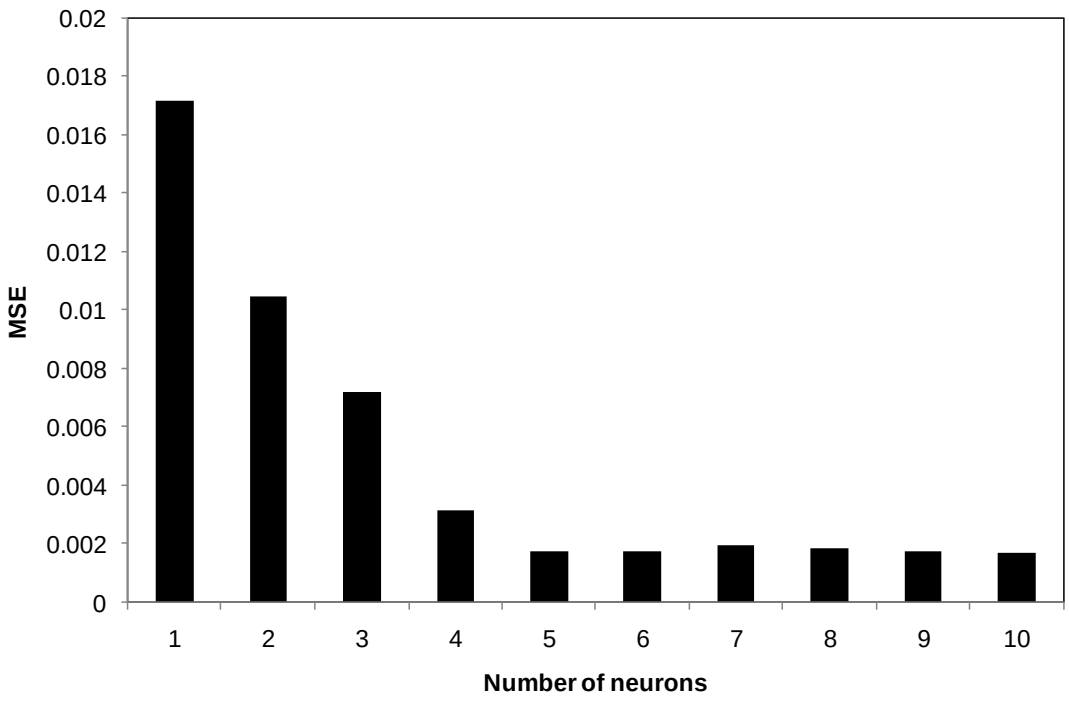

Figure 3. Optimization of number of neurons in relation to MSE.

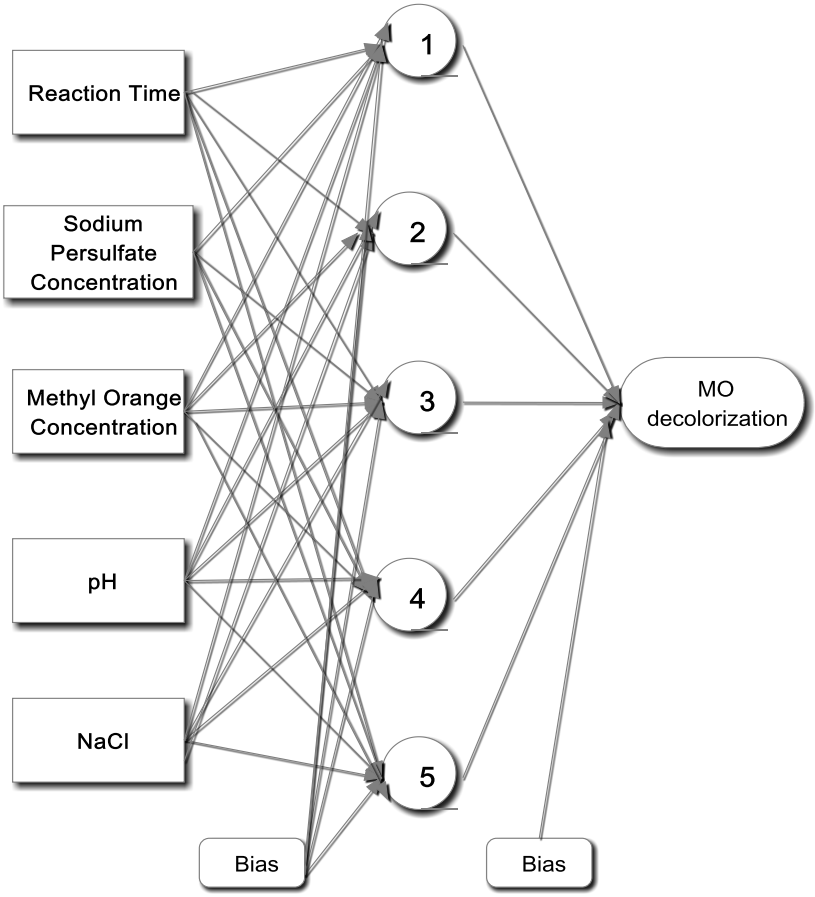

Figure 4. Structure of the optimized ANN used in this work.

(a)

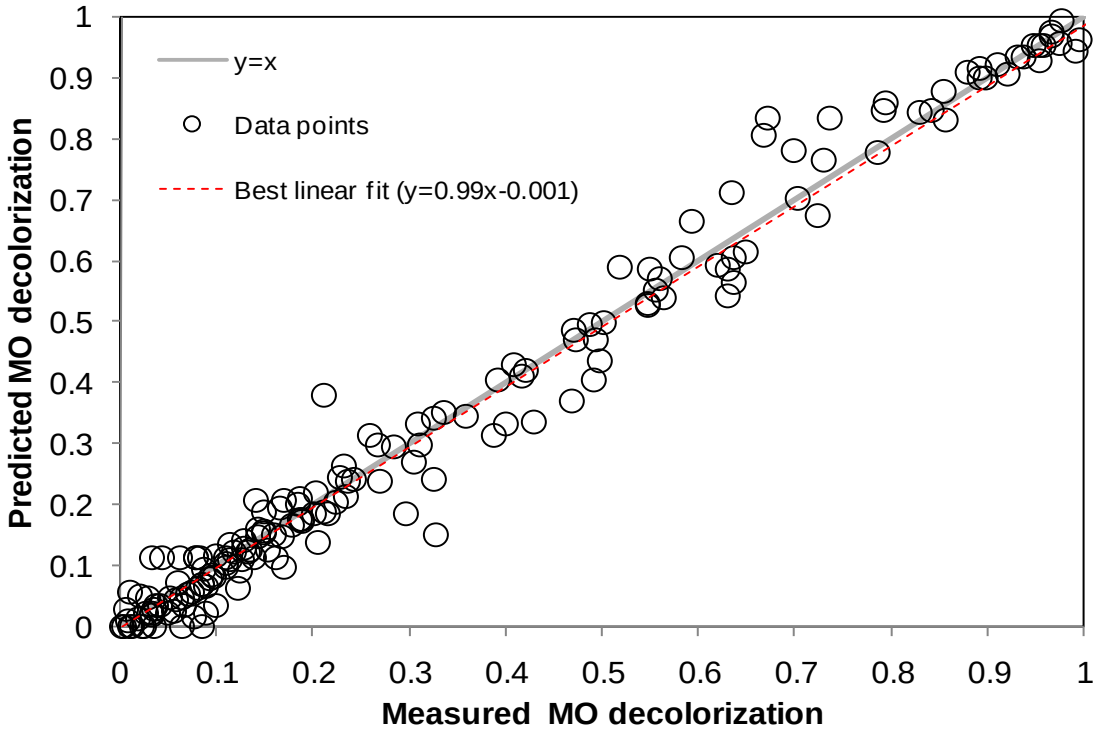

(b)

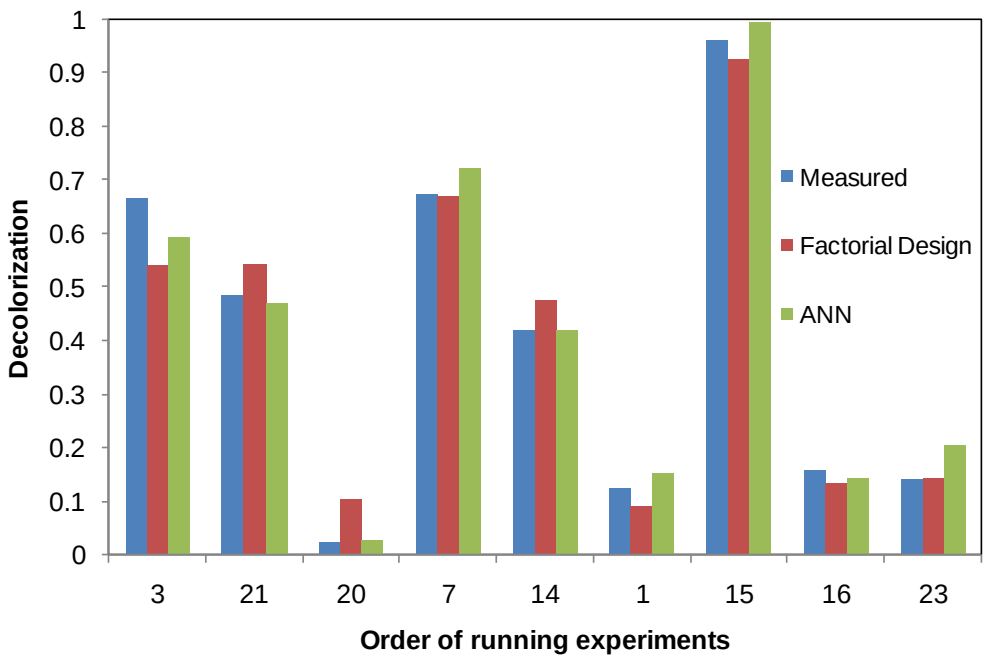

Figure 5. Comparison between measured and predicted values of the dependent variable. (a) ANN; (b) ANN versus factorial design.